Applied Physics B (2018) 124:101
https://doi.org/10.1007/s00340-018-6963-4

Applied Physics B
Lasers and Optics

Half-Watt average power femtosecond source spanning 3–8 μm based on subharmonic generation in GaAs

Viktor Smolski[1] · Sergey Vasilyev[1] · Igor Moskalev[1] · Mike Mirov[1] · Qitian Ru[2] · Andrey Muraviev[2] · Peter Schunemann[3] · Sergey Mirov[1,4] · Valentin Gapontsev[5] · Konstantin Vodopyanov[2]

Received: 30 January 2018 / Accepted: 24 April 2018

Abstract
Frequency combs with a wide instantaneous spectral span covering the 3–20 μm molecular fingerprint region are highly desirable for broadband and high-resolution frequency comb spectroscopy, trace molecular detection, and remote sensing. We demonstrate a novel approach for generating high-average-power middle-infrared (MIR) output suitable for producing frequency combs with an instantaneous spectral coverage close to 1.5 octaves. Our method is based on utilizing a highly-efficient and compact Kerr-lens mode-locked Cr^{2+}:ZnS laser operating at 2.35-μm central wavelength with 6-W average power, 77-fs pulse duration, and high 0.9-GHz repetition rate; to pump a degenerate (subharmonic) optical parametric oscillator (OPO) based on a quasi-phase-matched GaAs crystal. Such subharmonic OPO is a nearly ideal frequency converter capable of extending the benefits of frequency combs based on well-established mode-locked pump lasers to the MIR region through rigorous, phase- and frequency-locked down conversion. We report a 0.5-W output in the form of an ultra-broadband spectrum spanning 3–8 μm measured at 50-dB level.

1 Introduction

Laser frequency combs in the MIR spectral range are vital for many applications ranging from fundamental molecular spectroscopy and the study of molecular dynamics to multi-species trace gas sensing and hyperspectral imaging in the molecular fingerprint region. Additionally, many applications such as remote sensing and nonlinear comb spectroscopy require comb generators with a high average power and/or high power per comb tooth [1]. In the latter case, frequency combs with large mode spacing (GHz range) are of particular interest. MIR frequency combs can be generated directly from crystalline, fiber-based or quantum cascade mode-locked lasers, via difference frequency generation (DFG), optical parametric oscillators (OPOs), or in high-Q microresonators pumped by single-frequency MIR lasers [1].

In terms of frequency combs with a high average power in the molecular fingerprint wavelength range ($\lambda > 3$ μm), the best results so far have been achieved in OPO and DFG based systems. Adler and co-authors reported a high-power fully stabilized OPO-based MIR comb, where a singly-resonant linear-cavity OPO was synchronously pumped by a 10-W femtosecond (fs) 1.07-μm Yb-fiber laser. The OPO employed a 7-mm periodically poled lithium niobate (PPLN) crystal with a variable poling period; its center wavelength was continuously tunable from 2.8 to 4.8 μm and the maximum MIR power of 1.42 W was obtained at 3.2 μm center wavelength with an instantaneous bandwidth of 0.3 μm [2]. Cruz et al. produced high average power frequency combs based on DFG. The amplified fs pulses at 1.05 and 1.55 μm, seeded by the same oscillator (the average power in each of the beams was, respectively, 4 W and 140 mW), were mixed in a 3-mm-long MgO:PPLN crystal to produce

This article is part of the topical collection "Mid-infrared and THz Laser Sources and Applications" guest edited by Wei Ren, Paolo De Natale and Gerard Wysocki.

✉ Viktor Smolski
vsmolski@ipgphotonics.com

[1] IPG Photonics-Southeast Technology Center, Birmingham, AL 35211, USA

[2] CREOL, College of Optics and Photonics, Univ. Cent. Florida, Orlando, FL 32816, USA

[3] BAE Systems, P.O. Box 868, MER15-1813, Nashua, NH 03061, USA

[4] University of Alabama at Birmingham, Birmingham, AL 35294, USA

[5] IPG Photonics Corporation, Oxford, MA 01540, USA

Published online: 11 May 2018

tunable (2.6–5.2 μm) output at a 100 MHz repetition rate. The highest DFG average power of 500 mW was reported for the output that spanned 2.8–3.5 μm [3]. On the longer wavelength side, broadband two-optical-cycle MIR pulses with an average power of 100 mW at a 100 MHz repetition rate and the spectrum spanning 6.8–16.4 μm were obtained from a DFG source driven by a Yb:YAG thin-disc fs oscillator with a 90-W average power [4]. The authors used a 1-mm-thick $LiGaS_2$ (LGS) nonlinear crystal to produce a MIR output via self-mixing the spectral components of the same ultra-broadband pulse centered at $\lambda = 1.03$ μm.

A new technique suitable for generating ultra-broadband MIR frequency combs, based on a synchronously pumped degenerate OPO (also referred to as a subharmonic or frequency-divide-by-2 OPO), which rigorously both down-converts and dramatically augments the spectrum of a pump laser source, has been demonstrated [5, 6]. This technique proved to be suitable for generating broadband MIR combs using, as nonlinear material, periodically poled lithium niobate, orientation-patterned gallium arsenide (OP-GaAs) and orientation-patterned gallium phosphide (OP-GaP), combined with different pump lasers. These systems include Er–fiber pumped PPLN (comb span 2.5–3.8 μm) [5] and OP-GaP OPO (comb span 2.3–4.8 μm) [7], Tm-fiber pumped OP-GaAs OPO (comb span 2.6–6.1 μm) [8], and Cr^{2+}:ZnS-laser -pumped OP-GaAs OPO (comb span 3.6–5.6 μm) [9]. Such a device serves as an ideal frequency divider that is phase locked to the pump laser. The coherence properties of doubly resonant femtosecond OPOs were studied in detail in [10, 11], where sub-hertz relative linewidths between the pump and OPO comb teeth, as well as a clean division of pump carrier-envelope offset (CEO) frequency by 2 were experimentally demonstrated. Another attractive feature of subharmonic generators is the full recycling of the generated photons resulting in high conversion efficiency; for example, an optical conversion efficiency of 64% in a subharmonic OPO has been demonstrated in [12].

The choice of a pump laser is critical for an ultra-broadband subharmonic OPO and depends on the nonlinear optical crystal in use. One needs to take into account linear and multi-photon absorption, group velocity dispersion, and other properties. As a general remark, long pump wavelengths are beneficial since one can get deeper into MIR by generating a subharmonic. Recently, Watt-level mode-locked fs laser sources based on thulium-doped fibers at $\lambda \approx 1.95$ μm [13, 14], erbium-doped fluoride fibers at $\lambda \approx 2.8$ μm [15], Ho:YAG thin disks at $\lambda \approx 2.09$ μm [16], and transition-metal-doped II–VI semiconductors [17, 18], among which ZnS and ZnSe doped with Cr^{2+} ions (center $\lambda = 2.3$–2.4 μm) are most frequently used, have been demonstrated. The advantages of Cr:ZnS/ZnSe lasers include a very broad gain bandwidth that allows producing short (down to few optical cycles) pulses, the absence of excited state absorption, close to 100% quantum efficiency of fluorescence, and convenient pumping by erbium and thulium fiber lasers with a conversion efficiency in excess of 60%. Currently Cr:ZnS/ZnSe lasers enable producing up to 140 W of the output power when operated in the continuous-wave (CW) regime [19], more than 7 W of the average power in the mode-locked regime [20], and up to 1 GW of peak power in the regime of chirped-pulse amplification [21]. Cr:ZnS/ZnSe lasers have also proven to be very suitable for pumping MIR OPOs based on GaAs [9]. Specifically, due to low group dispersion of GaAs near the lasers' subharmonic frequencies (~ 5 μm) one can attain a very broad (up to 2 octaves) parametric gain bandwidth at degeneracy.

In this paper, we present a compact femtosecond MIR source with large, ~ 1 GHz, mode spacing that is based on a subharmonic OP-GaAs OPO and that delivers an ultra-broadband output spanning 3–8 μm with an average power of 0.5 W.

2 Cr^{2+}:ZnS laser setup

Due to their broad absorption and emission bands, Cr:ZnS and Cr:ZnSe are often referred to as 'Ti:sapphire of the middle-infrared'. Recent commercial availability of quality Cr:ZnS and Cr:ZnSe crystals, coupled with the convenience high power fiber lasers for optical pumping have stimulated rapid progress of fs Cr:ZnS and Cr:ZnSe lasers. Femtosecond oscillators based on all major mode-locking techniques have been implemented over the past decade, as reviewed in [22, 23].

In our design of the pump laser we rely on the Kerr-lens mode-locking technique [18, 20, 24, 25] as it allows for shorter pulses, higher power in comparison with, e.g. mode-locked lasers based on semiconductor saturable absorbers. We use X- folded linear resonators with an unconventional normal incidence (as opposed to Brewster's angle incidence used before) mounting of the AR coated polycrystalline gain elements. We avoid the use of prisms or plates for control of the chromatic dispersion and instead tailor the dispersion spectra of the optical coatings; we usually control second and third order dispersion within one-third of an octave. Cr:ZnS and Cr:ZnSe provide many possibilities for power and energy scaling of fs pulses centered near $\lambda = 2.35$ μm. Relatively high emission cross sections and long upper-state lifetimes of these materials enable extremely compact and robust single-pass amplifiers with unique output parameters, including: multi-Watt average power, multi-MW peak power (in the regime of amplified single pulses), broad spectral spans ($\Delta\lambda \approx 1.3$ μm at − 30 dB level), and a range of repetition rates (from kHz to GHz).

A schematic of our ultrafast Cr:ZnS laser source implemented for synchronous pumping of an OPO, is shown in

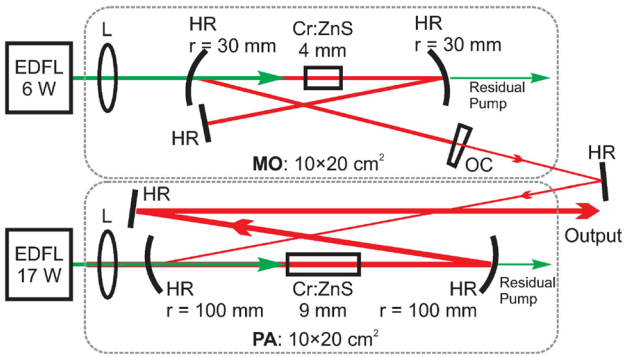

Fig. 1 Schematic of the ultrafast Cr^{2+}:ZnS laser source. *MO* Kerr-lens mode-locked Cr:ZnS master oscillator, *PA* single-pass full repetition rate Cr:ZnS power amplifier, *EDFL* fiber laser, *L* focusing lens, *HR* dielectric coated dispersive high reflectors, *OC* output coupler for Cr:ZnS laser radiation. All optical coatings are dispersion controlled

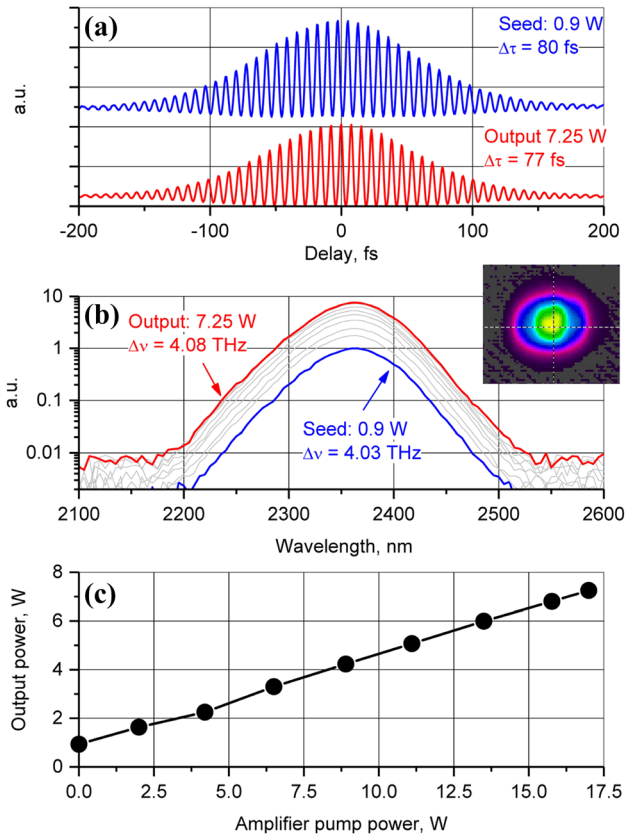

Fig. 2 Measured 2nd order autocorrelations (ACs), spectra, and the average power of MOPA pulses. **a** Initial AC (top, amplifier is off) is compared with the final AC (bottom, amplifier is on). Numbers near ACs show the pulse durations $\Delta\tau$ (estimated using sech^2 fit). **b** Initial spectrum (blue) normalized to unity; final spectrum (red) normalized to the optical power; grey lines show intermediate spectra, obtained during the gradual increase of pump power (all normalized to power). Numbers near the spectra show the output power and spectral bandwidth (FWHM). An insert in (**b**) shows the beam profile at a 7.25 W output power. Spectra were measured by a Princeton SP2150 monochromator with 150 g mm^{-1} grating and a Thorlabs PDA20H detector. **c** The average power of the fs Cr:ZnS MOPA pulses vs. pump power

Fig. 1. The system includes Kerr-lens mode-locked Cr:ZnS master oscillator at 2.35 μm central wavelength (MO) and a full repetition rate single-pass Cr:ZnS amplifier (PA). The fs MOPA is pumped by the radiation of off-the-shelf CW Er-doped fiber lasers (EDFLs) at $\lambda \approx 1.57$ μm.

The MO (PA) modules were equipped with 4 mm (9 mm) long AR coated polycrystalline Cr:ZnS gain elements with an ~16% (~2%) small signal transmission at 1.57 μm pump wavelength. The gain elements were cooled with room-temperature water. All dielectric mirrors were dispersion-controlled. Spatial mode-matching of the laser beams was implemented by optimization of the optical path length between the units. An inter-stage optical isolation was unnecessary. The fs Cr:ZnS MOPA was operated in a standard lab environment at 30–40% relative humidity (at room temperature).

The repetition rate of the MO was set to 0.9 GHz. This high repetition rate allowed us to reduce the length of the optical resonator to 17 cm and provided a good balance between the average and peak power of fs pulses, which is necessary for efficient pumping of an OPO. The footprints of the units are indicated in Fig. 1 and include the optical mounts but exclude the EDFA pumps.

The output characteristics of ultrafast Cr:ZnS MOPA are shown in Fig. 2. As can be seen, the amplifier fully preserves the spectral and temporal parameters of the seed pulses. We relied on the control software of our autocorrelator (A·P·E corporation) and used the sech^2 fit of the autocorrelation functions for evaluations of the pulse duration. We estimate the duration of the output pulses to be 77 fs (10 optical cycles) with the time-bandwidth product of 0.32.

Figure 2c shows a close-to-linear dependence of the output power vs. the EDFL pump power. We measured the average MIR power of 7.25 at 17 W pumping. Thus, high conversion efficiency of CW EDFL radiation to fs MIR pulses ($\eta = 37\%$) was combined with a high gain ($G = 8$) in our experiment. The obtained parameters correspond to 8.1 nJ energy and 100 kW peak power of pulses at a 0.9 GHz repetition rate.

The output beam profile, measured by a pyroelectric camera, is shown in the inset in Fig. 2b. The high quality of the output beam has allowed for efficient coupling of Cr:ZnS laser radiation to the OPO resonator. Thermal optical effects inside the gain element of Cr:ZnS amplifier induced some dependence of the output parameters of the Gaussian beam (size and divergence) on the output power. We used this dependence to fine-tune the spatial mode-matching between the laser beam at 2.35 μm and the OPO.

Our OPO experiments were carried out at 6-W maximum average power of the Cr:ZnS MOPA.

3 Frequency-divide-by-two OPO

The OPO design is similar to that described in [9, 26] with one major difference of a tenfold pulse repetition rate increase and the corresponding decrease of the resonator size. The OPO had a bow-tie ring resonator (Fig. 3) with a 34-cm optical roundtrip length matching the 0.9-GHz pump laser pulse repetition rate. It includes two off-axis gold-coated parabolic mirrors (OAP, off-axis angle 30°, apex radius 20 mm, effective focal length ≈ 10 mm), a dielectric coated input coupler for pump pulses (IC) on a 3 mm-thick YAG substrate, and a gold-coated plane high reflector (HR). The dielectric coating of the input coupler provided high transmission (> 85%) at 2.35 µm pump wavelength and high reflection (~ 95%) for the 3–7 µm OPO band, centered at 4.7-µm half-subharmonic of the pump laser.

As a nonlinear gain element we used an uncoated 0.5-mm thick OP-GaAs crystal with a quasi-phase matching period of $\Lambda = 88$ µm. The OP-GaAs crystal was grown by a combination of molecular-beam and hydride vapor phase epitaxial growth at BAE systems [27]. The sample was mounted at Brewster's angle and oriented such that all the beams inside the crystal propagated along < 110 > direction of GaAs, while polarizations of all the participating beams, namely the pump beam and the OPO signal and idler beams were parallel to < 111 > direction. A thin ZnSe wedge with 1° apex angle was installed inside the OPO resonator (see Fig. 3) for two purposes: (i) dispersion control and (ii) as a broadband output coupler for signal/idler waves. The net dispersion of the OPO resonator was adjusted by varying the wedge thickness, while the outcoupling was adjusted by tilting the wedge away from Brewster's angle. Thus, the OPO had three output ports, as shown in Fig. 3. The main signal at the subharmonic wavelength was equally split between the Outputs #1 and #2; the depleted pump (and a small fraction of the subharmonic) was transmitted through the input coupler (the Output #3).

In the process of the OPO alignment, the distance between the OPO parabolic mirrors, as well as the position of the OP-GaAs nonlinear gain crystal were adjusted to achieve the best spatial mode overlap between the OPO eigenmode and the pump laser beam. The size of the pump beam (after the mode-matching optics) at the first OAP mirror inside the OPO cavity was estimated to be $w = 0.66$ mm ($1/e^2$ intensity radius) resulting in the focused beam size of $w_0 = 11$ µm. Taking into account the oblique incidence at Brewster's angle, we estimate the pump peak intensity inside the OP-GaAs crystal, at the maximum 6 W of average power used in our experiment, to be 13 GW/cm^2. At this level of peak intensities, we did not see any negative effects of the three-photon absorption in the GaAs crystal induced by the 2.35-µm pump, in full accordance with [28].

The OPO was enclosed in a Plexiglas box and purged with dry nitrogen. The footprint of the OPO setup is indicated in Fig. 3 and includes the optical mounts without the mode-matching optics. The overall footprint of the setup was about 1 m^2, however, only ~ 0.06 m^2 was occupied by the lasers and the rest was used to provide the optical paths for the spatial mode-matching. Furthermore, we mostly used the standard optical mounts and did not put any special effort into the footprint reduction. Nonetheless, we believe that the whole source, consisting of the fs Cr:ZnS MOPA and the OPO, can be easily packaged to a shoebox-size of 0.25 m^2.

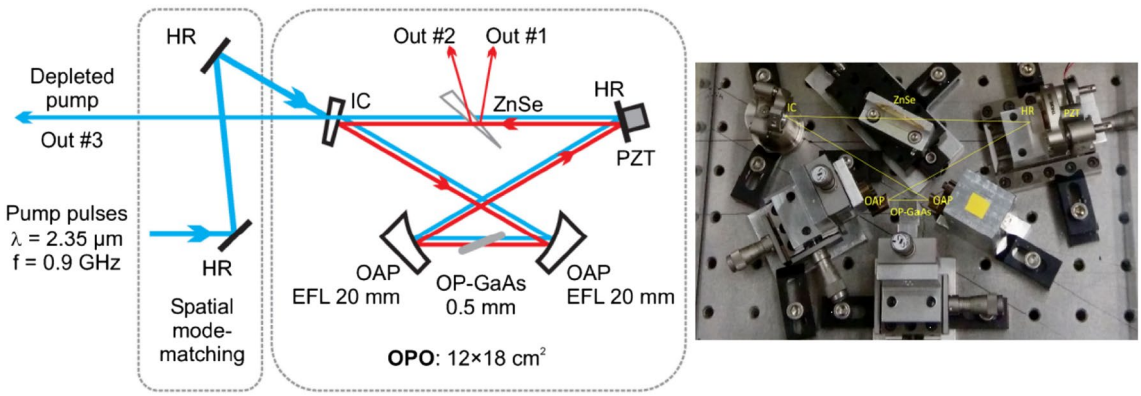

Fig. 3 Schematic of the synchronously pumped subharmonic OPO. *HR* gold coated flat mirror, *OAP* gold coated parabolic mirrors, *IC* output/input coupler, *PZT* piezo transducer, *ZnSe* wedge with 1° apex angle for dispersion control and OPO outcoupling. Inset: photo of the OPO setup

4 Results

The doubly resonant OPO is interferometrically sensitive to the cavity length adjustment and operates at a few individual cavity resonances (peaks) spaced, in terms of the roundtrip length, approximately by half of the OPO central wavelength [5]. Scanning of the OPO resonator length by a piezo transducer (PZT) around a synchronous pumping optimum is illustrated in Fig. 4. We have selected for our measurements a peak that corresponded to the broadest degenerate spectrum and the highest average output power.

With a minimal OPO outcoupling (ZnSe wedge was at Brewster's angle), the OPO threshold was measured to be 162 mW, while the pump depletion that was measured at higher pump powers (several times above threshold) was as high as 90% (we used the auxiliary Output #3 for this measurement). Then, we gradually increased the OPO outcoupling and the pump power, and made several rounds of the OPO resonator's optimization. The highest OPO output power was obtained at 16% outcoupling (combined from two beams) and at the average pump power of 6 W. Although we were able to actively lock the OPO cavity length to one of the resonances (via PZT actuator and an electronic servo loop [5]), the available pump power at 2.35 µm was sufficiently high to observe thermal self-stabilization (self-locking for tens of seconds) of the OPO resonator cavity to the pump pulse train, similar to [29]. The measured average power of the OPO was > 0.2 W per each reflection from the ZnSe wedge (Outputs 1 and 2 in Fig. 3). Taking into account the losses in the long-pass ($\lambda > 3$ µm) filter, which we used before the power meter, we derived the overall MIR power in excess of 0.5 W. The measured pump depletion at this 'optimal' OPO outcoupling was lower, about 40–60% (hence we believe the parameters of the OPO can be further improved).

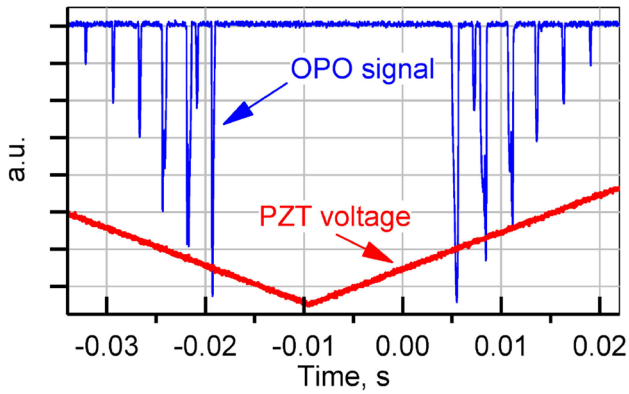

Fig. 4 Detected OPO peaks (inverted) vs. time. The length of the OPO resonator is scanned at 10 Hz rate by a piezo transducer. The consecutive peaks of the OPO generation are separated by half of the OPO central wavelength (2.35 µm) in terms of the roundtrip length change

Our OPO spectral measurements were performed with a grating monochromator (Princeton SP2150, 150 gr/mm grating), a cooled (77K) mercury cadmium telluride (MCT) detector (Teledyne Judson), and a set of long-pass filters (LP3000, LP4500, and LP5000 from Spectrogon). We did not post-process the spectrum to account for spectral dependences of the diffraction efficiency of the grating, sensitivity of the detector and filters' transmission. We measured the output spectrum, while the OPO resonator length was dithered near its optimal work point by a piezo actuator, by detecting the MCT signal and demodulating it by a lock-in amplifier. The acquired spectrum is shown in Fig. 5. Also shown in Fig. 5 is the spectrum of the pump, as well as the reflectivity curve of the input coupler IC. As can be seen, the subharmonic OPO spectrum spans from 3 to 8 µm (− 50 dB level), which is in full accordance with our calculations based on the OP-GaAs parametric gain bandwidth, IC reflectivity curve, and the roundtrip intracavity group delay dispersion of the OPO resonator. Finally, the spectral brightness of our system of ~ 120 µW per mode near 4 µm

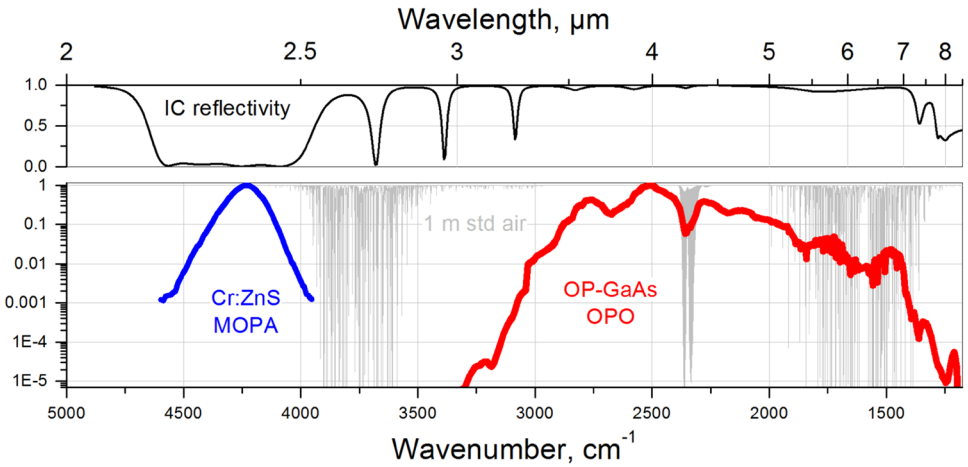

Fig. 5 The broadest normalized measured spectrum of the degenerate OPO (bottom right) as compared to the normalized pump spectrum (bottom left). Transmission of 1 m of standard air is shown in gray. The top panel shows theoretical reflectivity of the input coupler

compares favorably with that of other high-power mid-IR systems operating at lower (~ 100 MHz) repetition rates, e.g. 22 μW per mode near 3.2 μm [2], 5 μW near 3 μm [3], 3.5 μW near 11 μm [4], and 2 μW near 5.4 μm [30].

5 Conclusion

We demonstrate a compact high-power (0.5 W) GHz-repetition-rate MIR source with a broad instantaneous spectral span exceeding one octave (3–8 μm). In this system, we used readily available and wall-plug-efficient CW EDFLs to pump the Cr:ZnS 2.35-μm MOPA system, which in turn pumped the OPO. Overall, we achieved a 2.6% conversion efficiency from the 1.57-μm EDFL source to the broadband femtosecond MIR output. Our further steps will include phase locking of the pump laser to produce, via coherent frequency division, a phase-stable ultra-broadband MIR frequency comb suitable for real-world applications.

Acknowledgements KLV would like to thank the Office of Naval Research (ONR) (grant N00014-15-1-2659) and Defense Advanced Research Projects Agency (DARPA) (grant W31P4Q-15-1-0008) for the financial support.

References

1. A. Schliesser, N. Picqué, and T.W. Hänsch, Mid-infrared frequency combs. Nat. Photon. **6**, 440–449 (2012)
2. F. Adler, K.C. Cossel, M.J. Thorpe, I. Hartl, M.E. Fermann, J. Ye, Phase-stabilized, 1.5 W frequency comb at 2.8–4.8 μm. Opt. Lett. **34**, 1330–1332 (2009)
3. F.C. Cruz, D.L. Maser, T. Johnson, G. Ycas, A. Klose, F.R. Giorgetta, I. Coddington, S.A. Diddams, Mid-infrared optical frequency combs based on difference frequency generation for molecular spectroscopy. Opt. Express **23**, 26814 (2015)
4. I. Pupeza, D. Sánchez, J. Zhang, N. Lilienfein, M. Seidel, N. Karpowicz, T. Paasch-Colberg, I. Znakovskaya, M. Pescher, W. Schweinberger, V. Pervak, E. Fill, O. Pronin, Z. Wei, F. Krausz, A. Apolonski, J. Biegert, High-power sub-two-cycle mid-infrared pulses at 100 MHz repetition rate. Nat. Photon. **9**, 721–724 (2015)
5. N. Leindecker, A. Marandi, R.L. Byer, K.L. Vodopyanov, Broadband degenerate OPO for mid-infrared frequency comb generation. Opt. Express **19**, 6296–6302 (2011)
6. K.L. Vodopyanov, S.T. Wong, R.L. Byer, "Infrared frequency comb methods, arrangements and applications. U.S. patent (2013). 8,384,990 (February 26) (2013)
7. Q. Ru, Z.E. Loparo, X. Zhang, S. Crystal, S. Vasu, P.G. Schunemann, K.L. Vodopyanov, Self-referenced octave-wide subharmonic GaP optical parametric oscillator centered at 3 μm and pumped by an Er-fiber laser. Opt. Lett. **42**, 4756–4759 (2017)
8. V.O. Smolski, H. Yang, S.D. Gorelov, P.G. Schunemann, K.L. Vodopyanov, Coherence properties of a 2.6–7.5 μm frequency comb produced as a subharmonic of a Tm-fiber laser. Opt. Lett. **41**(7), 1388–1391 (2016)
9. V.O. Smolski, S. Vasilyev, P.G. Schunemann, S.B. Mirov, K.L. Vodopyanov, Cr:ZnS laser-pumped subharmonic GaAs optical parametric oscillator with the spectrum spanning 3.6–5.6 μm. Opt. Lett. **40**, 2906–2908 (2015)
10. A. Marandi, N. Leindecker, V. Pervak, R.L. Byer, K.L. Vodopyanov, Coherence properties of a broadband femtosecond mid-IR optical parametric oscillator operating at degeneracy. Opt. Express **20**, 7255–7262 (2012)
11. K.F. Lee, C. Mohr, J. Jiang, P.G. Schunemann, K.L. Vodopyanov, M.E. Fermann, Midinfrared frequency comb from self-stable degenerate GaAs optical parametric oscillator. Opt. Express **23**, 26596–26603 (2015)
12. A. Marandi, K.A. Ingold, M. Jankowski, R.L. Byer, Cascaded half-harmonic generation of femtosecond frequency combs in the mid-infrared. Optica **3**, 324–327 (2016)
13. J. Bethge, J. Jiang, C. Mohr, M. Fermann, I. Hartl, Optically referenced Tm-fiber-laser frequency comb, in Lasers, Sources, and Related Photonic Devices (Optical Society of America, 2012), paper AT5A.3 (2012)
14. C. Gaida, M. Gebhardt, F. Stutzki, C. Jauregui, J. Limpert, A. Tünnermann, Thulium-doped fiber chirped-pulse amplification system with 2 GW of peak power. Opt. Lett. **41**, 4130–4133 (2016)
15. S. Duval, M. Olivier, V. Fortin, M. Bernier, M. Piché, R. Vallée, 23-kW peak power femtosecond pulses from a mode-locked fiber ring laser at 2.8 μm. In: Proc. SPIE 9728, 972802, (2016)
16. J. Zhang, K.F. Mak, S. Gröbmeyer, D. Bauer, D. Sutter, V. Pervak, F. Krausz, O. Pronin, Generation of 220 fs, 20 W pulses at 2 μm from Kerr-lens mode-locked Ho:YAG thin-disk oscillator. In: Conference on Lasers and Electro-Optics, OSA Technical Digest (online) (Optical Society of America, 2017), paper SM1I.6
17. S. Mirov, V. Fedorov, D. Martyshkin, I. Moskalev, M. Mirov, S. Vasilyev, Progress in mid-IR lasers based on Cr and Fe-doped II–VI chalcogenides. IEEE J. Sel. Topics Quant. Electron. **21**, 1601719 (2015)
18. S. Mirov, I. Moskalev, S. Vasilyev, V. Smolski, V. Fedorov, D. Martyshkin, J. Peppers, M. Mirov, A. Dergachev, and V. Gapontsev, Frontiers of mid-IR lasers based on transition metal doped chalcogenides. Submitted for publication. In: IEEE J. Sel. Topics in Quantum Electron. (2018)
19. S. I.Moskalev, M. Mirov, S. Mirov, V. Vasilyev, A. Smolski, V. Zakrevskiy, Gapontsev, 140 W Cr:ZnSe laser system. Opt. Express **24**(18), 21090–21104 (2016)
20. S. Vasilyev, I. Moskalev, M. Mirov, V. Smolski, S. Mirov, V. Gapontsev, Ultrafast middle-IR lasers and amplifiers based on polycrystalline Cr:ZnS and Cr:ZnSe. Opt. Mat. Express **7**, 2636–2650 (2017)
21. E. Slobodchikov, L.R. Chieffo, K.F. Wall, High peak power ultrafast Cr:ZnSe oscillator and power amplifier. In: Proc. SPIE 9726, Solid State Lasers XXV: technology and devices, 972603, (March 16, 2016)
22. T. Sorokina, E. Sorokin, Femtosecond Cr^{2+}-based lasers. IEEE J. Sel. Top. Quant. Electron. **21**(1), 1601519 (2015)
23. S. Vasilyev, M. Mirov, V. Gapontsev, Kerr-lens mode-locked femtosecond polycrystalline Cr^{2+}:ZnS and Cr^{2+}:ZnSe lasers. Opt. Express **22**(5), 5118–5123 (2014)
24. S. Vasilyev, I. Moskalev, M. Mirov, S. Mirov, V. Gapontsev, Three optical cycle mid-IR Kerr-lens mode-locked polycrystalline Cr^{2+}:ZnS laser. Opt. Lett. **40**(21), 5054–5057 (2015)
25. S. Vasilyev, I. Moskalev, M. Mirov, S. Mirov, V. Gapontsev, Multi-Watt mid-IR femtosecond polycrystalline Cr^{2+}:ZnS and Cr^{2+}:ZnSe laser amplifiers with the spectrum spanning 2.0–2.6 μm. Opt. Express **24**(2), 1616–1623 (2016)
26. Q. Ru, K. Zhong, N. Lee, Z. Loparo, P. Schunemann, S. Vasilyev, S. Mirov, K. Vodopyanov, Instantaneous spectral span of 2.85–8.40 μm achieved in a Cr:ZnS laser pumped subharmonic OPO. In: Proc. SPIE 10088, Nonlinear Frequency Generation and Conversion: Materials and Devices XVI, 1008809, (2017)
27. P.G. Schunemann, K.T. Zawilski, L.A. Pomeranz, D.J. Creeden, P.A. Budni, Advances in nonlinear optical crystals for mid-infrared coherent sources. J. Opt. Soc. Am. **33**, D36 (2016)

28. W.C. Hurlbut, Y.-S. Lee, K.L. Vodopyanov, P.S. Kuo, and M.M. Fejer, Multiphoton absorption and nonlinear refraction of GaAs in the mid-infrared. Opt. Lett. **32**, 668 (2007)
29. K. Lee, C. Mohr, J. Jiang, P. Schunemann, K. Vodopyanov, M. Fermann, Midinfrared frequency comb from self-stable degenerate GaAs optical parametric oscillator. Opt. Express **23**, 26596–26603 (2015)
30. L. Maidment, P.G. Schunemann, D.T. Reid, Molecular fingerprint-region spectroscopy from 5 to 12 μm using an orientation-patterned gallium phosphide optical parametric oscillator. Opt. Lett. **41**, 4261 (2016)